

## Supramolecular assemblies of the *Ascaris suum* major sperm protein (MSP) associated with amoeboid cell motility

Karen L. King<sup>1,2</sup>, Murray Stewart<sup>2</sup> and Thomas M. Roberts<sup>1,\*</sup>

<sup>1</sup>Department of Biological Science, Florida State University, Tallahassee, FL 32306-3050, USA

<sup>2</sup>MRC Laboratory of Molecular Biology, Hills Rd, Cambridge CB2 2QH, UK

\*Author for correspondence

### SUMMARY

Sperm of the nematode, *Ascaris suum*, are amoeboid cells that do not require actin or myosin to crawl over solid substrata. In these cells, the role usually played by actin has been taken over by major sperm protein (MSP), which assembles into filaments that pack the sperm pseudopod. These MSP filaments are organized into multi-filament arrays called fiber complexes that flow centripetally from the leading edge of the pseudopod to the cell body in a pattern that is intimately associated with motility. We have characterized structurally a hierarchy of helical assemblies formed by MSP. The basic unit of the MSP cytoskeleton is a filament formed by two subfilaments coiled around one another along right-handed helical tracks. In vitro, higher-order assemblies (macrofibers) are formed by MSP

filaments that coil around one another in a left-handed helical sense. The multi-filament assemblies formed by MSP in vitro are strikingly similar to the fiber complexes that characterize the sperm cytoskeleton. Thus, self-association is an intrinsic property of MSP filaments that distinguishes these fibers from actin filaments. The results obtained with MSP help clarify the roles of different aspects of the actin cytoskeleton in the generation of locomotion and, in particular, emphasize the contributions made by vectorial assembly and filament bundling.

Key words: amoeboid locomotion, cytoskeleton, electron microscopy, filament, nematoda

### INTRODUCTION

Amoeboid cells crawl over substrata by extending filament-packed pseudopods. Generally locomotion is thought to be mediated through a cytoskeleton based on actin and a spectrum of accessory proteins (see, for example, Bray, 1992; Condeelis, 1993; Gerisch et al., 1991; Hartwig and Kwaitkowski, 1991; Pollard, 1986; Pollard and Cooper, 1986; Stossel, 1993). However, because of the multitude of cellular functions performed by the actin cytoskeleton (see Bray, 1992), the precise identification of those properties that are directly associated with cell motility has not been straightforward. In this context, the extraordinary simplicity and specialization of motility in the amoeboid sperm of nematodes may offer advantages in identifying some of the basic mechanical molecular mechanisms underlying locomotion (see Heath, 1992).

Spermatozoa of the nematode, *Ascaris suum*, crawl like amoebae by extending a filament-packed pseudopod. These sperm display classic features of amoeboid locomotion such as membrane protrusion, ruffling and cytoskeletal flow, but lack the actin-based cytoskeleton generally associated with this type of locomotion (reviewed by Roberts et al., 1989). Instead, *Ascaris* sperm contain a simple cytoskeleton based primarily on major sperm protein, MSP (Sepsewol et al., 1989). MSP filaments assemble preferentially at the leading edge of the

sperm pseudopod and are organized into long, multi-filament fiber complexes. These filamentous arrays are linked to the pseudopod plasma membrane at protrusions called villipodia and extend back to the junction between the cell body and pseudopod (Sepsewol et al., 1989). As sperm crawl forward, these complexes flow back towards the cell body due to filament assembly at the leading edge and disassembly at the rear of the pseudopod (Roberts and King, 1991; Sepsewol et al., 1989; Sepsewol and Taft, 1990).

Vectorial assembly of MSP filaments and their arrangement into fiber complexes are integral features of the locomotion of *Ascaris* sperm. The rate of filament assembly, for example, is coupled so tightly to the speed of locomotion that, regardless of how fast the cell is crawling, cytoskeletal assembly keeps pace with locomotion (Sepsewol et al., 1989; Roberts and King, 1991). Moreover, the villipodial protrusions that lead the forward advance of the sperm form only where fiber complexes are linked to the membrane. Because the behavior of the cytoskeleton appears to dictate the speed and direction of sperm locomotion, understanding sperm motility requires detailed knowledge of the structure of MSP; the arrangement of MSP molecules within filaments; and the organization of these filaments in the cytoskeleton.

*Ascaris* MSP has two 14 kDa isoforms ( $\alpha$ - and  $\beta$ -), each containing 126 residues (King et al., 1992). Their amino acid

sequences differ at only four positions and are not homologous with other cytoskeletal proteins. Although crystals of MSP that are suitable for X-ray crystallographic analysis have been produced (Stewart et al., 1993), a detailed structure of the MSP molecule has not yet been determined. MSP assembles into filaments that have a characteristic substructure of axial dots (King et al., 1992). There is, however, little information about the structure of these filaments or of other supramolecular assemblies, such as fiber complexes, formed by MSP. Therefore, we have examined MSP filaments and investigated how they assemble *in vitro* into higher-order structures analogous to those observed in the sperm cytoskeleton. We show here that MSP has a striking capacity to form a distinctive hierarchy of macromolecular assemblies both *in vivo* and *in vitro*. Moreover, these MSP assemblies give clues as to which properties of the actin-based cytoskeleton are important in generating conventional amoeboid locomotion.

## MATERIALS AND METHODS

### Examination of native filaments

*Ascaris* males were collected and their sperm isolated and activated as described by King et al. (1992). Sperm were pipetted onto carbon-coated, 200-mesh nickel grids rendered hydrophilic by glow discharge. Grids were checked by light microscopy for actively crawling sperm before lysis by treatment with HKB buffer (50 mM HEPES, 65 mM KCl, 10 mM NaHCO<sub>3</sub>, pH 7.2) containing 0.5% Triton X-100. MSP filaments in the demembrated cells were prevented from disassembling by fixation in 1% glutaraldehyde within 2-3 seconds after lysis. These specimens were washed with several drops of HKB buffer, negatively stained with 1% aqueous uranyl acetate, and air dried.

### MSP purification

*Ascaris* MSP was prepared essentially as described (King et al., 1992). Briefly, sperm homogenate was centrifuged at 10,000 *g* for 15 minutes then at 100,000 *g* for 45 minutes. MSP was partially purified from the supernatant by size exclusion chromatography on a Sephadex G-75 superfine column (2.5 cm × 90 cm) equilibrated in HKN buffer (50 mM HEPES, 65 mM KCl, 10 mM NaCl, pH 7.2). MSP-enriched fractions were collected and isoforms separated by cation exchange chromatography on Sepharose S - fast flow equilibrated with phosphate buffer (8 mM NaH<sub>2</sub>PO<sub>4</sub>, 2 mM Na<sub>2</sub>HPO<sub>4</sub>, pH 6.0). Typically 30-40 mg of protein was loaded onto the column, which then was washed with 5 volumes of equilibration buffer. To elute  $\alpha$ - and  $\beta$ -MSP, the salt concentration was increased stepwise from 0 to 25 mM and the pH was increased from 6.0 to 6.5. Beta-MSP eluted first in phosphate buffer with 15 mM NaCl, pH 6.0, followed by alpha-MSP in phosphate buffer with 25 mM NaCl, pH 6.5.

### Electron microscopy

For negative staining, filaments were prepared by diluting purified  $\beta$ -MSP to a final concentration of 0.2 mM (3 mg/ml) with 30% ethanol in phosphate buffer. This solution, which contained numerous MSP filaments, was placed in a small, shallow cap and maintained at 10°C. A carbon film on freshly cleaved mica was floated onto the surface of this filament solution (Valentine et al., 1968), washed with 27% ethanol in 10 mM phosphate buffer, pH 6, then stained with 3.5% uranyl acetate in 27% ethanol. The carbon film was picked up from underneath with rhodium-coated, 400-mesh, copper grids. Filaments for shadowing were prepared in a similar manner, except that after staining with 3.5% uranyl acetate in 27% ethanol, filaments adsorbed onto the carbon film were transferred to a solution of 27% ethanol in distilled water (total volume >100 ml). A rhodium-coated, 400-mesh,

copper grid was placed on the carbon film and then carefully lifted off. Grids were then shadowed unidirectionally with platinum at a nominal angle of 10 degrees in an Edwards Coating System E306A using a Cressington EB 602 PC electron-beam gun and power supply.

Both negatively stained preparations and shadowed filaments were examined in either JEOL 1200 EX or Philips CM12 electron microscopes operated at 80 or 100 kV. Images were recorded on Kodak SO163 film at nominal magnifications between ×25,000 and ×100,000.

Filament diameter and substructure repeat distances were measured directly from calibrated prints. All values are means ± standard deviation with the number of observations.

## RESULTS

### MSP filaments

The MSP filament system in the sperm pseudopod disassembles rapidly when the cell is lysed, unless stabilizing agents such as polyethylene glycol (PEG) or fixatives such as glutaraldehyde are added to the lysis solutions (King et al., 1992). We found that assembly of MSP filaments *in vitro* in phosphate buffer required MSP at concentrations greater than 3 mM (45 mg/ml). Because MSP filaments are highly labile (King et al., 1992), preservation of this material for examination by EM required fixation with glutaraldehyde, which caused aggregation of high concentrations of unpolymerized MSP. These aggregates could not be removed by washing and, thus, gave high backgrounds of amorphous material in preparations of negative-stained filaments (Fig. 1). We therefore found it most convenient to examine the structure of MSP filaments formed in the presence of water-miscible alcohols, such as methanol and ethanol, at concentrations similar to those that have been used many times to crystallize proteins for X-ray diffraction studies (McPherson, 1985). Previous studies showed that these alcohol-induced filaments have a structure that is indistinguishable from that of native filaments in sperm lysed with Triton X-100 and rapidly fixed with glutaraldehyde (King et al., 1992). Moreover, assembly in 30% ethanol occurs at a critical concentration of 0.2 mM (3 mg/ml) MSP (King et al., 1992),



**Fig. 1.** Negatively stained filaments assembled by incubating  $\beta$ -MSP at a concentration of 45 mg/ml in phosphate buffer, pH 6.7, and fixed in 2.5% glutaraldehyde. The heavy background due to aggregates produced by the high concentration of unpolymerized MSP obscured fine detail in the filaments. Bar, 100 nm.

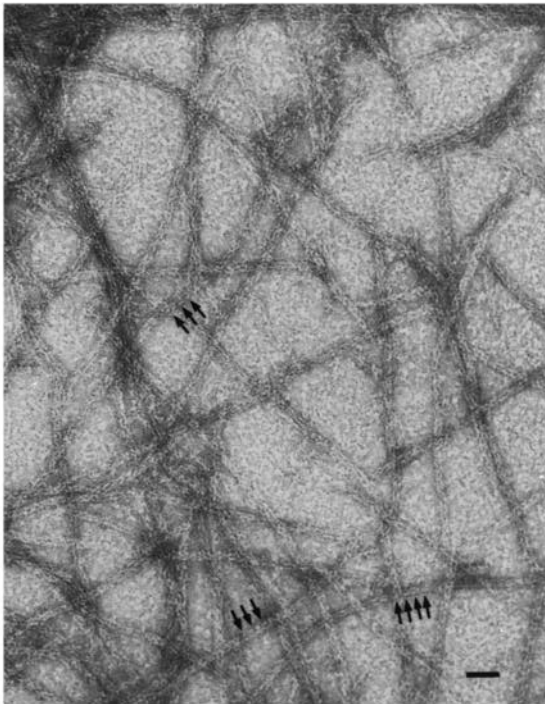


**Fig. 2.** Negatively stained filaments assembled by incubating  $\beta$ -MSP in 30% ethanol. Because the background has been reduced filament fine structure is now clear. The axial repeat of dots spaced roughly at 11 nm intervals characteristic of these filaments is indicated by the series of arrows. Bar, 40 nm.

which substantially reduced the background in electron micrographs due to unpolymerized monomers (Fig. 2). An important feature of the ethanol-induced polymerization of MSP was its reversibility. When ethanol was removed from the preparation, the MSP filaments depolymerized rapidly. Critically, filaments reassembled when ethanol was added back. This reversibility

indicated that the ethanol had not denatured MSP or induced polymerization in some aberrant way.

As previously shown (King et al., 1992), filaments produced by the ethanol-induced polymerization of MSP were  $11 \text{ nm} \pm 2 \text{ nm}$  in diameter ( $n=20$ ) in negatively stained preparations and had a pattern of dots along the filament axis (Fig. 2). The axial spacing between dots was slightly irregular but averaged  $11 \text{ nm} \pm 2 \text{ nm}$  ( $n=20$ ). This pattern was observed in both native filaments and those produced in vitro (King et al., 1992). Short filaments were seen occasionally in some preparations. Most filaments, however, were several micrometers in length and usually followed a gently curving path.

MSP filaments themselves were constructed from subfilaments that could often be distinguished at the ends of frayed filaments (Fig. 3, arrows). These subfilament strands sometimes followed a sinusoidal path, suggesting that they probably had a helical substructure. Often short individual subfilaments could also be seen in the background (Fig. 3, arrowheads) of negatively stained preparations. We did not ever observe more than two subfilaments at a frayed filament end, indicating that the filaments were constructed from two subfilaments coiled around one another. Filaments with frayed ends were found relatively frequently, indicating that the bonds between MSP subunits were probably stronger along the two subfilaments in each filament than between them.

Filaments shadowed unidirectionally with platinum/carbon (Fig. 4) were roughly 12–14 nm in diameter, although the precise value varied according to the shadowing direction. Shadowed filaments had a characteristic pattern of diagonal striations extending from the lower left to the upper right-hand side of the filament (Fig. 4). The axial spacing between striations was  $10 \text{ nm} \pm 1 \text{ nm}$  ( $n=10$ ). Because shadowing contrasts only the upper surfaces of helices, it enables the paths followed by subfilaments to be observed directly (see Stewart, 1988). The direction of the striations in Fig. 4 shows that the subfilaments followed right-handed helical tracks with pitch of about

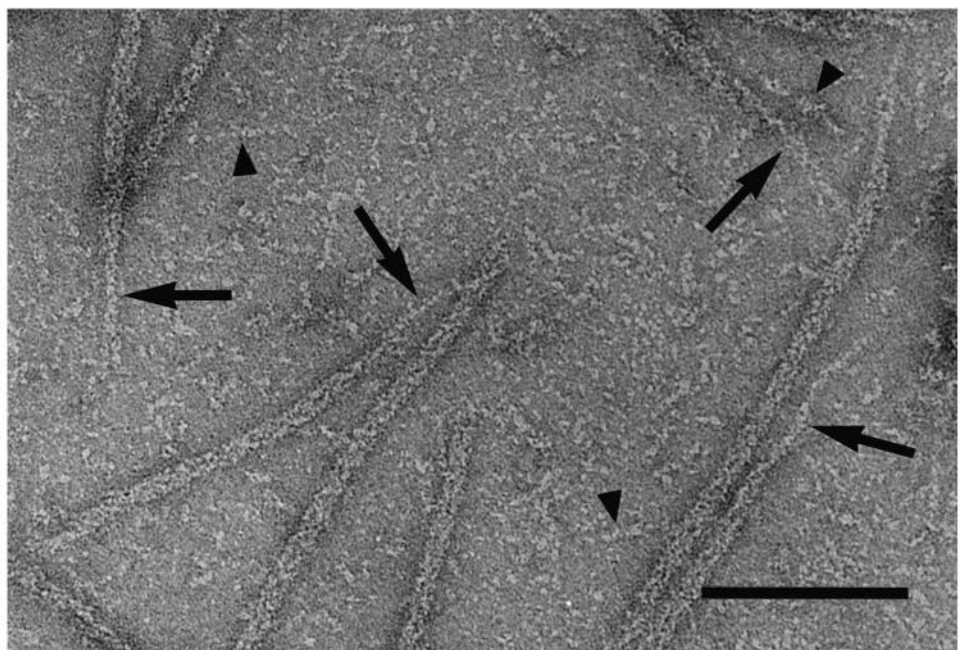


**Fig. 3.** Negatively stained field of  $\beta$ -MSP filaments showing frayed ends. Single subfilaments can be seen emerging from several filaments in this field (arrows) and close inspection indicates that the subfilaments themselves sometimes tend to follow a somewhat sinusoidal path. Often individual short subfilaments can be seen in the background (arrowheads). Bar, 100 nm.

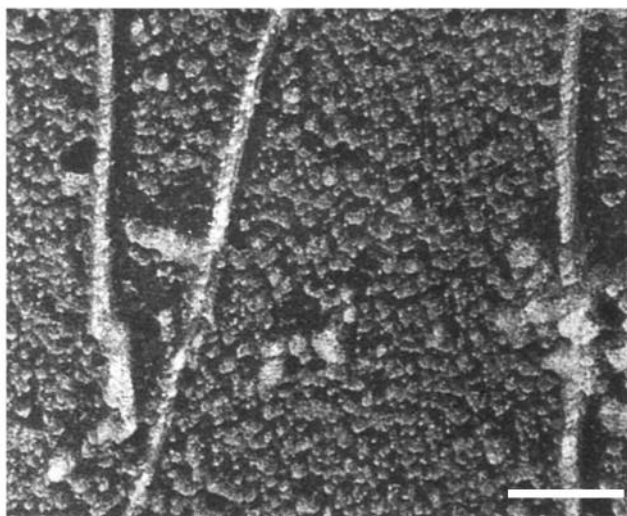


**Fig. 4.**  $\beta$ -MSP filaments shadowed unidirectionally with platinum/carbon. Diagonal striations extend from the lower left to the upper right of the filaments and show the right-handed helical tracks followed by subfilaments. Bar, 100 nm.

20 nm (because the pitch of a two-stranded helical structure is twice the spacing between striation; see Stewart, 1988).

### Macrofibers

In addition to single filaments, many ethanol-derived preparations contained larger-diameter aggregates formed by filaments wrapped around one another (Figs 5, 6). These rope-like macrofibers were more numerous in preparations formed by incubating MSP in ethanol for longer periods (2-3 minutes), whereas single filaments were more often found in preparations sampled after only a 30 second incubation. Negatively stained macrofibers (Fig. 5) had a characteristic braided appearance. As a consequence of the large depth of focus of

the electron microscope, patterns from the top and bottom of macrofibers were in focus simultaneously and so were superimposed in these images. This superimposition of all the different structural levels in the macrofibers created a moiré pattern, making the determination of the precise macromolecular structure of macrofibers, by simple inspection, extremely difficult. However, shadowing overcame this problem because, in these images, only the pattern from the top of the filament was visible (Fig. 6). The images of shadowed macrofibers showed clearly that they were composed from a number of filaments that followed left-handed helical tracks (diagonal striations from the top left to the bottom right of the macrofiber). Moreover, sometimes individual filaments could be seen splitting off from macrofibers when they splayed apart at their ends (Fig. 5D,E). Macrofibers in both negatively stained and shadowed preparations were easily distinguishable from isolated filaments because of their greater diameter. Macrofibers were heterogeneous in size, ranging from 20 to 30 nm in diameter, because they contained different numbers of filaments. Fig. 7 shows a histogram of the number of filaments per macrofiber. Three-stranded macrofibers were most common, but the strand number varied substantially and some contained as many as five distinguishable filaments.

In addition to macrofibers, the filaments formed during alcohol-induced assembly *in vitro* sometimes associated to form much larger aggregates. In some instances filaments and macrofibers were interwoven to form mats in which they crossed at a variety of angles to form a meshwork (Fig. 8A). Alternatively, filaments were sometimes aligned parallel to one another to form a sheet or raft analogous to the way logs align themselves floating down a river. Fig. 8B shows a negatively stained filament raft. MSP filaments within the rafts displayed the same axial repeat seen in individual filaments and were somewhat straighter. However, close inspection of images of negatively stained filaments indicated a lack of axial register in the rafts, because in adjacent filaments the pattern of axial dots spaced were not aligned (Fig. 8B, arrows).

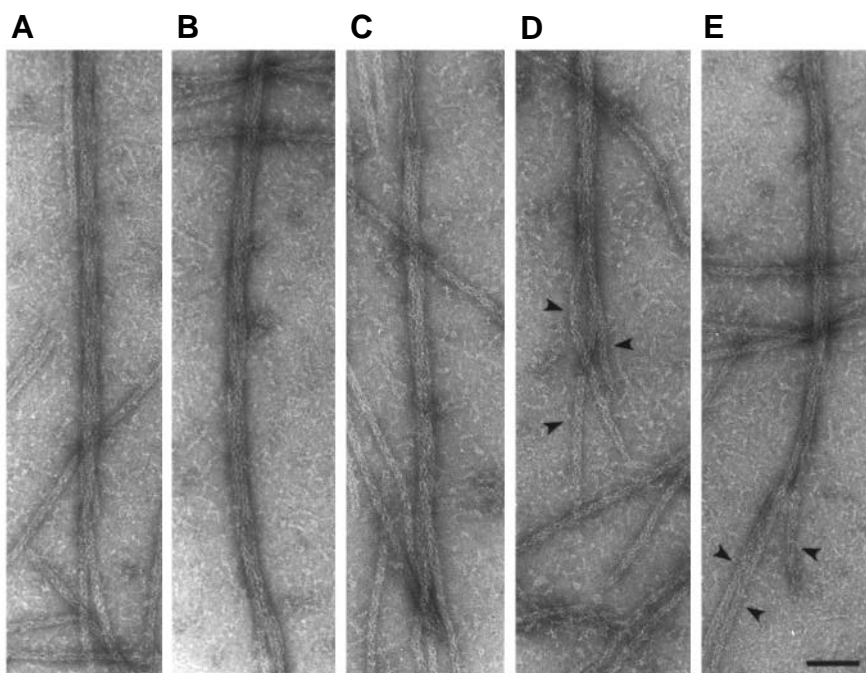


**Fig. 5.** Negatively stained macrofibers assembled by incubating  $\beta$ -MSP in 30% ethanol for 3 minutes. (A,B,C). Coiling of filaments around one another in the macrofiber can be seen clearly when viewed at a glancing angle down the long axis of the macrofiber. (D,E) Two macrofibers with frayed ends from which three filaments can be seen protruding (arrowheads). Bar, 50 nm.

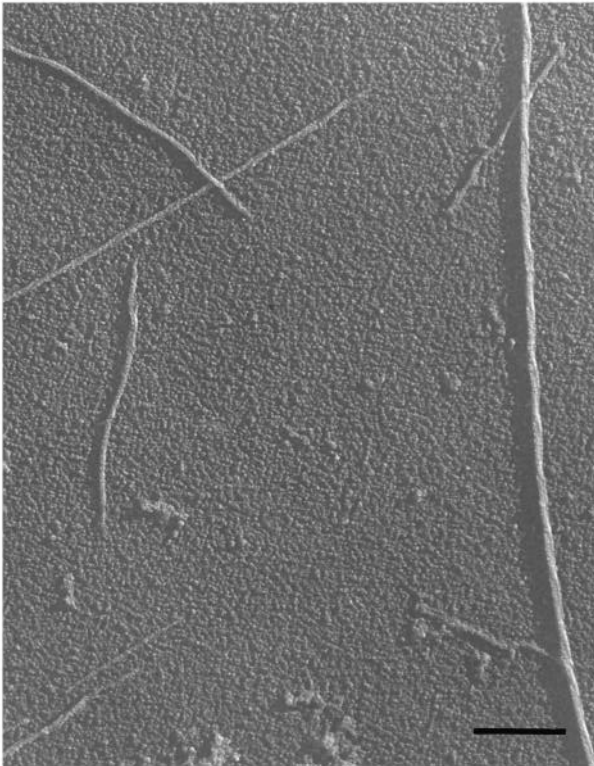


**Fig. 6.** Preparations of macrofibers produced by incubating  $\beta$ -MSP for 2 minutes after addition of ethanol to 30%. Shadowed unidirectionally with platinum/carbon. Diagonal striations can be seen in several of the macrofibers when viewed from the side. Note the number of different sizes of macrofiber present in a single preparation. Bar, 200 nm.

### Fiber complexes

Large filamentous superstructures, analogous in many ways to the ethanol-induced macrofibers, are also present in the sperm pseudopod (Sepsenwol et al., 1989). Here, MSP filaments are grouped into large fiber complexes (150–200 nm) that extend from the leading edge of the pseudopod to the cell body. Fig. 9 shows part of a negatively stained whole-cell mount in which the fiber complexes within a pseudopod can be seen. Filaments were tightly packed at the center of these complexes. Some extended out to interweave with filaments from adjacent fiber complexes, linking them together (Fig. 9; see also Sepsenwol et al., 1989). Fiber complexes are often branched and, during locomotion, move as a single unit to the rear of the pseudopod (Sepsenwol et al., 1989; Roberts and King, 1991).

Fig. 10 shows a portion of a negatively stained fiber complex at high magnification. The fiber complex is composed of filaments that associate with each other through different types of interactions to form filament aggregates resembling those seen *in vitro*. Some filaments coil around one another, some filaments associate side-to-side, and others are arranged into orthogonal networks or mats. The filament coils of different sizes found throughout the fiber complex (Fig. 10, insets) resembled the macrofibers formed *in vitro*. Filament ends within the fiber complexes were often obscured, so we were unable to determine filament lengths precisely, although they appeared to be at least several micrometers long. All filaments

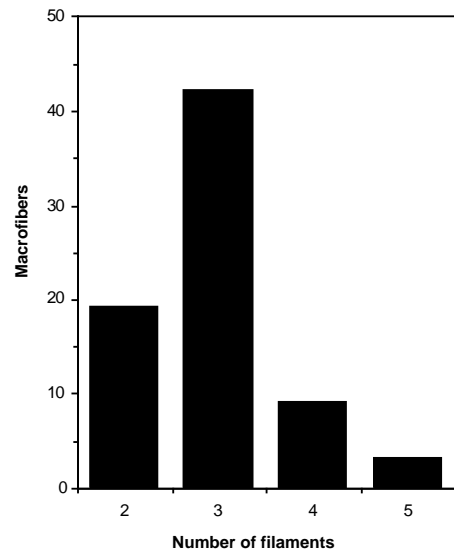


**Fig. 7.** Number of filaments per macrofiber. Macrofibers were formed by incubating  $\beta$ -MSP in 30% ethanol for 3 minutes. The number of filaments per macrofiber was determined by examining macrofibers that were uncoiled at their end so that individual filaments that comprised the macrofiber could be counted reliably. Macrofibers were most commonly composed of three MSP filaments.

within negatively stained fiber complexes were, however, 10–12 nm in diameter (Fig. 10).

## DISCUSSION

The MSP filament system in nematode sperm is analogous to the actin cytoskeleton in other amoeboid cells (Roberts et al., 1989; Ward, 1986). In *Ascaris* sperm, vectorial assembly produces filaments along the leading edge that are organized into three-dimensional arrays and flow rearward as the cell progresses. The filaments are arranged into fiber complexes and the rate of fiber complex assembly is equal to the rate of sperm locomotion (Roberts and King, 1991; Sepsenwol et al., 1989). To understand the relationship between the formation of these multi-filament arrays and force production during sperm locomotion, we have characterized MSP filaments and the supramolecular structures that they form.

### MSP macromolecular assemblies

MSP forms four distinct macromolecular assemblies: subfilaments, filaments, macrofibers and fiber complexes (see Fig. 10). Individual MSP filaments are composed of two subfilaments wrapped around each other along right-handed helices of pitch about 20 nm. Isolated filaments are about 11 nm in diameter and, in electron micrographs, sometimes have single or separated subfilaments protruding from their ends (Figs 2 and 3). Furthermore, MSP filaments polymerized *in vitro* associate to form larger helical macrofibers in the absence of accessory proteins (Figs 5 and 6). The structure of the macromolecular assemblies formed by MSP is analogous in many ways to a rope that consists of a number of fibers twisted around to form a strand. Strands then coil around one another

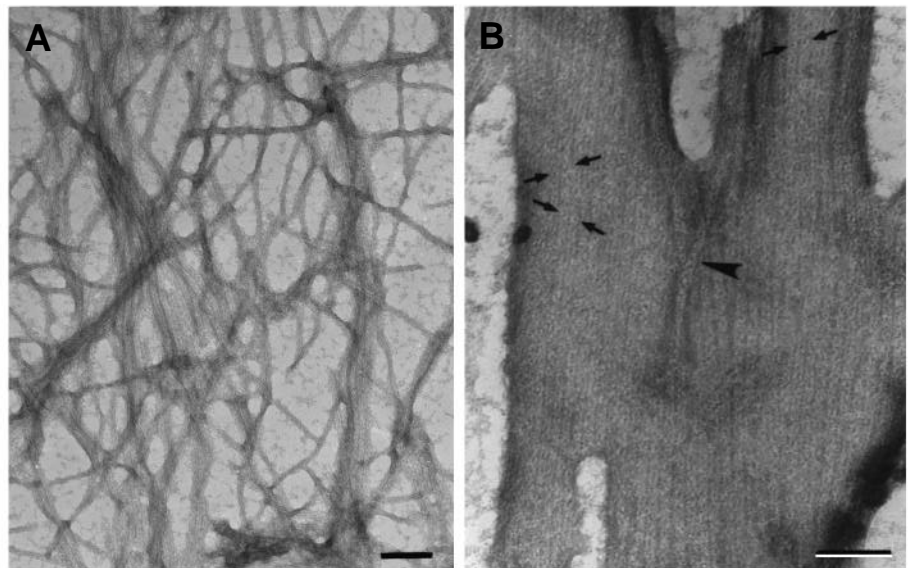


**Fig. 8.** (A) Negatively stained mat of filaments, resembling fiber complexes, generated by incubating  $\beta$ -MSP in 30% ethanol for 5 minutes. Multi-filament coils intertwine to form a network. Bar, 100 nm. (B) Negatively stained  $\beta$ -MSP filament raft formed in 30% ethanol. Filaments in the raft contain dots spaced roughly at 11 nm intervals and an individual filament can be seen emerging from the raft (arrowhead). Arrows mark regions in the raft where filaments are not in axial register as indicated by non-alignment of the dots along adjacent filaments. Bar, 50 nm.

to form the rope. Likewise, individual MSP polypeptide chains polymerize to form subfilaments; two subfilaments twist around each other to form filaments; and these filaments wrap around each other to form macrofibers or fiber complexes (see Fig. 11). The organization of filaments in macrofibers parallels in many respects the way in which MSP filaments interact to form fiber complexes *in vivo* (Figs 6 and 8). We cannot rule out entirely the possibility that the ethanol used for MSP polymerization *in vitro* may promote the association of filaments into larger aggregates, but several lines of evidence suggest that this is unlikely. For example, filaments formed in ethanol are indistinguishable from native filaments (King et al., 1992) and ethanol-induced polymerization is reversible, indicating that aberrant interactions have not been induced. Moreover, the organization of filaments in lysed sperm resembles filament arrays formed *in vitro*: filaments in fiber complexes coil around one another in the same way as observed in macrofibers, and although ethanol-induced mats did not display all of the organizational features of *in vivo* fiber complexes, filaments and macrofibers were interwoven and crossed each other much like the arrangement of native filaments in fiber complexes (compare Figs 8 and 10; see also Sepsenwol et al., 1989).

### Comparison of MSP and actin

Although MSP and actin appear to have analogous roles in amoeboid motility, the similarities between the two proteins and the macromolecular assemblies they form are only superficial. Although both actin and MSP are globular proteins, MSP is three times smaller than actin and shares no sequence similarity (King et al., 1992). Both self-assemble into fibrous polymers, but whereas actin polymerization can be modulated by divalent cations and involves ATP (Pollard, 1986, 1990), neither cation nor nucleotide dependence has been demonstrated for MSP polymerization (King et al., 1992). Although both actin and MSP filaments are based on right-handed, two-stranded helices, the long helical pitch of actin is about 72 nm, whereas the subfilaments in the MSP filaments follow helical tracks of pitch about 20 nm. Interactions between MSP subunits within a subfilament appear stronger than interactions between molecules in adjacent subfilaments. Single subfila-

ments are sometimes found at the ends of filaments and occasionally two subfilaments uncoil to form 'split ends'. Actin filaments form single strands only when filaments are destabilized (Bremer et al., 1991).

Actin and MSP also differ in the way that they form higher-order assemblies. With MSP the formation of both filaments and macrofibers, as well as mats of filaments, proceeded

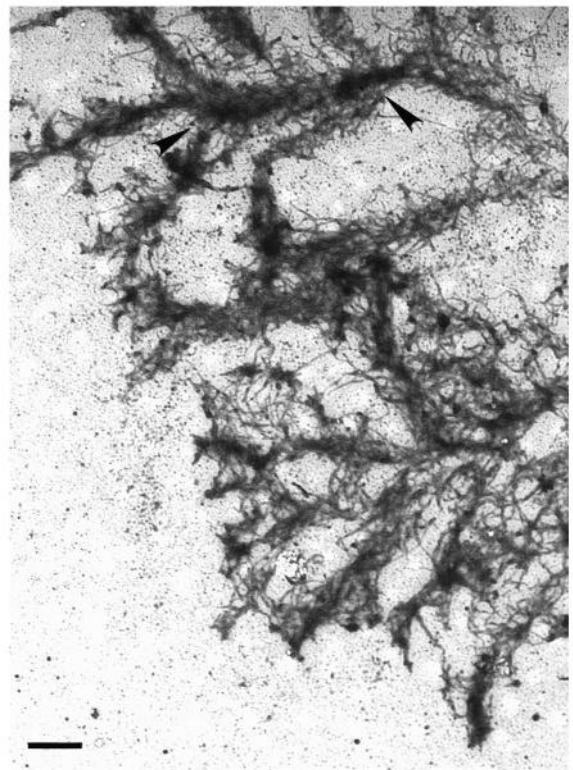


**Fig. 9.** Negatively stained fiber complexes at the leading edge of the pseudopod of a spermatozoon that has been extracted with Triton X-100 and then chemically fixed with glutaraldehyde. The fiber complexes often are branched (arrowheads) and filaments are more dense at the core of the fiber complex than at the edges. Bar, 300 nm.

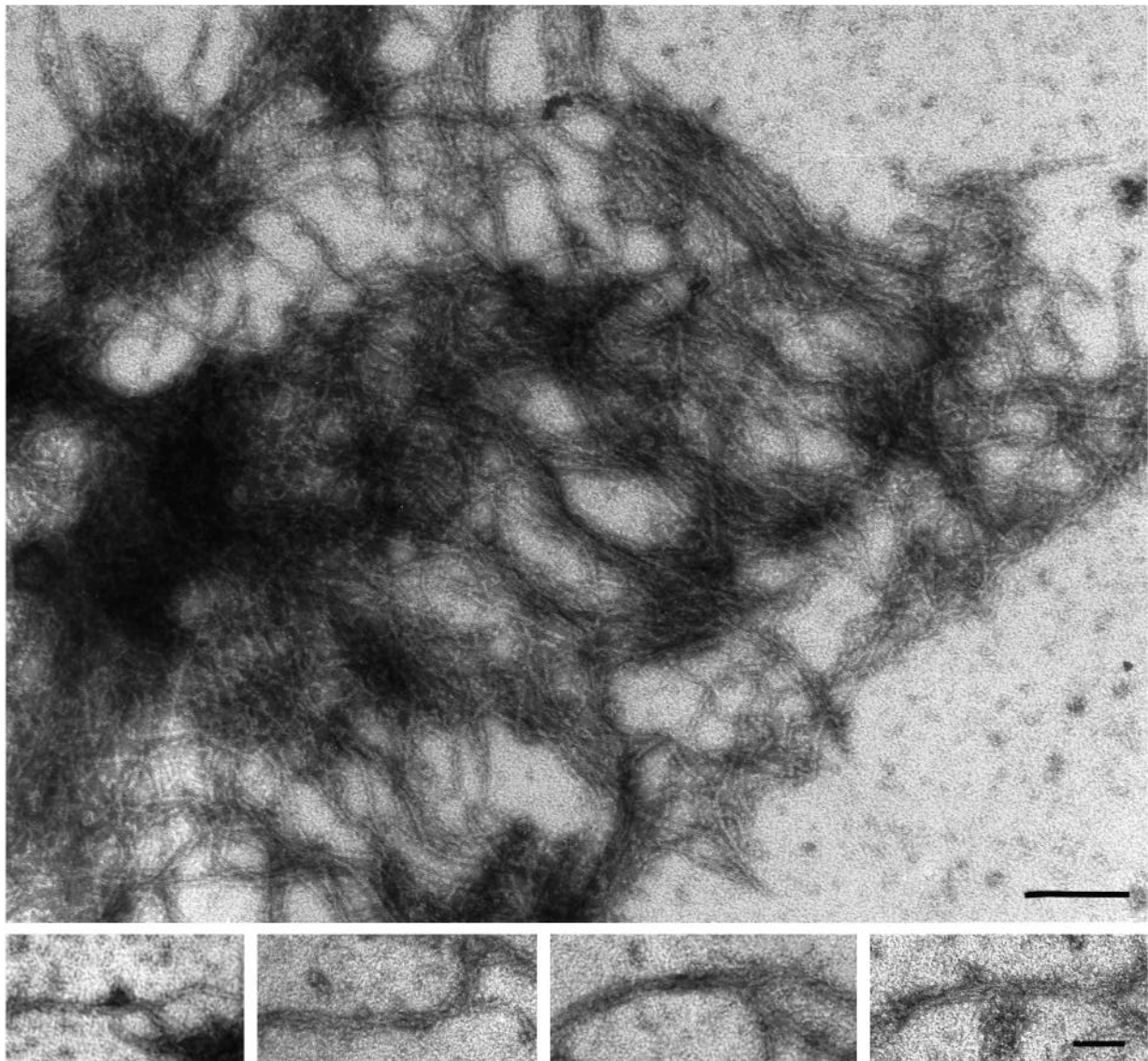


**Fig. 10.** Portion of a negatively stained fiber complex. The fiber complex contains numerous filament coils and bundles as well as individual filaments. Several types of interaction link filaments together: filaments coil around one another; lie parallel to one another; and cross each other to form filament networks. Bar, 200 nm. Insets: multi-filament bundles within fiber complexes formed by filaments associating together. Bar, 100 nm.

without accessory proteins. Although self-association of MSP filaments has only been documented *in vitro*, the similarities between the aggregates formed *in vivo* and *in vitro* suggest that filament aggregation *in vivo* may also not require accessory proteins. This contrasts with actin, where bundles are produced by accessory proteins (Bray, 1992).

#### Implications for actin-based amoeboid motility

Although actin has a central role in amoeboid motility in conventional eukaryotic cells, the precise mechanism by which locomotion is produced has been difficult to define because of the diversity of roles actin fulfills. In addition to locomotion, actin has a structural cytoskeletal role and is involved in such diverse cellular processes as cytokinesis, phagocytosis, organelle movement, and possibly vesicle transport (see, Bray, 1992). Indeed, the functional versatility of the actin system has

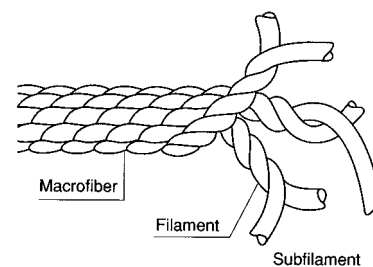


**Fig. 11.** Schematic illustration of the levels of coiling observed with MSP *in vitro*. Filaments are formed by two subfilaments that coil round one another following right-handed helical paths. Several filaments (most commonly three, as shown here) coil round one another following left-handed helical paths to produce macrofibers. To aid interpretation, the helical pitch of both filaments and macrofibers have been foreshortened.

made it difficult to define which properties of the actin cytoskeleton are essential for cellular locomotion.

Vectorial assembly of actin is generally accepted to play a vital role in amoeboid motility (Condeelis, 1993; Gerish et al., 1991; Luna and Hitt, 1992; Pollard, 1990; Stossel, 1993; Theirot and Mitchison, 1991, 1992). However, the role of filament networks and bundles is less clear. Although bundling or crosslinking proteins have sometimes been associated with changes in motility (Cox et al., 1992; Cunningham et al., 1992), molecular genetics experiments in which such proteins were deleted have not always produced severe impairment of cell motility (Brink et al., 1990; Cox et al., 1992; Noegel and Schleicher, 1991; Witke et al., 1992). It is possible that any of a number of proteins may be able to crosslink or bundle filaments (Bray and Vasiliev, 1989; Noegel and Schleicher, 1991), and so removal of any one of them may not, in itself, cause a decisive alteration in locomotion. Thus, it has been difficult to establish unequivocally that these proteins are necessarily associated with locomotion and not with some other role of the actin cytoskeleton.

The striking similarity between actin- and MSP-based cell locomotion, at least at the light microscopy level (Roberts and King, 1991; Sepsenwol et al., 1989; Sepsenwol and Taft, 1991), indicates that, although their components differ, the fundamental operating principles of the locomotive machinery are shared. Comparison of the two systems thus has a powerful potential for identifying mechanistic features that are necessary or sufficient for locomotion. Because they do not undergo phagocytosis, cytokinesis or vesicle transport, or display other cytoskeletal functions, these sperm allow the locomotive machinery to be examined independently of many of the other roles that complicate analysis in actin-based amoeboid systems.

In crawling sperm, both vectorial assembly and filament bundling are intimately associated with locomotion, and indeed the rates of both filament assembly and fiber complex formation are identical to that of cellular translocation (Roberts and King, 1991; Sepsenwol et al., 1989). The relationship among these processes is also seen in sperm incubated in weak acids where the cytoskeleton disassembles and the protrusions on the pseudopod surface disappear. Removal of the acidifying agents results in immediate reassembly of filaments along the pseudopod membrane, reorganization of these filaments into short fiber complexes, and simultaneous formation of new protrusions associated with each nascent fiber complex (Roberts and King, 1991). The ability of MSP to assemble into multi-filament arrays in vitro also suggests that filament bundling is important for sperm motility. This property could, in fact, simplify cytoskeletal assembly by reducing, or even eliminating, the need for accessory proteins to connect filaments into larger assemblies.

Because the sperm cytoskeleton is used primarily for locomotion, any intrinsic property of its principal component, MSP, is likely to be indispensable to translocation of the cell. Thus, the intrinsic ability of MSP to assemble into multi-filament arrays clearly identifies this property as an important component of MSP-based locomotion in *Ascaris* sperm. By analogy, therefore, these results also provide compelling evidence for assigning filament crosslinking a key role in actin-based systems. Formation of actin and MSP filaments into higher-order assemblies could influence motility in at least two

ways, which are not mutually exclusive and indeed may be synergistic. Filament bundles and networks would be stiffer than isolated filaments (Janmey, 1991; Stossel, 1993), and thus would provide a more rigid scaffold against which filaments could push to facilitate pseudopod extension. Such multi-filament arrays would also exert greater frictional forces on the cytoplasm to provide an anchor for the forces involved in pseudopod extension. Although additional experiments will be needed to completely exclude involvement of motor proteins, these observations raise the possibility that vectorial assembly and fiber complex formation alone may be sufficient for protrusion and locomotion.

We thank Missouri Lee, Charles Davis and Lawrence LeClaire for collection of *Ascaris*, Gregory Roberts for worm dissection, and Juliane Essig for MSP purification. This work was supported by NIH grant GM 29994 to T.M.R., NATO CRG 910264 to M.S., and Sigma Xi Grant-in-Aid of Research to K.L.K.

## REFERENCES

- Bray, D. and Vasiliev, J. (1989). Networks from mutants. *Nature* **338**, 203-204.
- Bray, D. (1992). *Cell Movements*. Garland Publishing, New York, NY.
- Bremer, A., Milloning, R. C., Sutterlin, R., Engel, A., Pollard, T. P. and Aebi, U. (1991). The structural basis for the intrinsic disorder of the F-actin filament: the lateral slipping model. *J. Cell Biol.* **115**, 689-703.
- Brink, M., Gerish, G., Isenberg, G., Noegel, A., Segall, J., Wallraff, E. and Schleicher, M. (1990). A *Dictyostelium* mutant lacking an F-actin cross-linking protein, the 120 kD gelation factor. *J. Cell Biol.* **111**, 1477-1489.
- Condeelis, J. (1993). Life at the leading edge: the formation of cell protrusions. *Annu. Rev. Cell Biol.* **9**, 411-444.
- Cox, D., Condeelis, J., Wessels, D., Soll, D., Kern, H. and Knecht, D. (1992). Targeted disruption of the ABP-120 gene leads to cells with altered motility. *J. Cell Biol.* **116**, 943-955.
- Cunningham, C. C., Gorlin, J. B., Kwiatkowski, D. J., Hartwig, J. H., Janmey, P. A., Byers, H. R. and Stossel, T. P. (1992). Actin-binding protein requirement for cortical stability and efficient locomotion. *Science* **255**, 325-327.
- Gerisch, G., Noegel, A. A. and Schleicher, M. (1991). Genetic alteration of proteins in actin-based motility systems. *Annu. Rev. Physiol.* **53**, 607-628.
- Hartwig, J. H. and Kwiatkowski, D. J. (1991). Actin-binding proteins. *Curr. Opin. Cell Biol.* **3**, 87-97.
- Heath, J. P. (1992). A worm's eye view of cell motility. *Curr. Biol.* **2**, 301-303.
- Janmey, P. A. (1991). Mechanical properties of cytoskeletal polymers. *Curr. Opin. Cell Biol.* **2**, 4-11.
- King, K. L., Stewart, M., Roberts, T. M. and Seavy, M. (1992). Structure and macromolecular assembly of two isoforms of the major sperm protein (MSP) from the amoeboid sperm of the nematode, *Ascaris suum*. *J. Cell Sci.* **101**, 847-857.
- Luna, E. and Hitt, A. (1992). Cytoskeleton-plasma membrane interactions. *Science* **258**, 955-964.
- McPherson, A. (1985). Crystallization of macromolecules: general principles. *Meth. Enzymol.* **114**, 112-120.
- Noegel, A. A. and Schleicher, M. (1991). Phenotypes of cells with cytoskeletal mutations. *Curr. Opin. Cell Biol.* **3**, 18-26.
- Pollard, T. D. (1986). Mechanism of actin filament self-assembly and regulation of the process by actin-binding proteins. *Biophys. J.* **49**, 49-151.
- Pollard, T. D. and Cooper, J. A. (1986). Actin and actin-binding proteins. A critical evaluation of mechanisms and functions. *Annu. Rev. Biochem.* **55**, 987-1035.
- Pollard, T. D. (1990). Actin. *Curr. Opin. Cell Biol.* **2**, 33-40.
- Roberts, T. M., Sepsenwol, S. and Ris, H. (1989). Sperm motility in nematodes: crawling movement without actin. In *The Cell Biology of Fertilization* (ed. H. Schatten and G. Schatten), pp. 41-60. Academic Press, Inc., San Diego.
- Roberts, T. M. and King, K. L. (1991). Centripetal flow and directed reassembly of the major sperm protein (MSP) cytoskeleton in the amoeboid sperm of the nematode, *Ascaris suum*. *Cell Motil. Cytoskel.* **20**, 228-241.

- Sepsenwol, S., Ris, H. and Roberts, T. M.** (1989). A unique cytoskeleton associated with crawling in the amoeboid sperm of the nematode, *Ascaris suum*. *J. Cell Biol.* **108**, 55-66.
- Sepsenwol, S. and Taft, S. J.** (1990). In vitro induction of crawling in the amoeboid sperm of the nematode parasite, *Ascaris suum*. *Cell Motil. Cytoskel.* **15**, 99-110.
- Stewart, M.** (1988). Computer image processing of electron micrographs of biological structures with helical symmetry. *J. Electron Microsc. Techn.* **9**, 325-358.
- Stewart, M., King, K. L. and Roberts, T. M.** (1993). Crystallization of the motile major sperm protein (MSP) of the nematode, *Ascaris suum*. *J. Mol. Biol.* **232**, 298-300.
- Stossel, T.** (1993). On the crawling of animal cells. *Science* **260**, 1086-1094.
- Theriot, J. A. and Mitchison, T. J.** (1991). Actin filament dynamics in locomoting cells. *Nature* **352**, 126-131.
- Theriot, J. A. and Mitchison, T. J.** (1992). The nucleation-release model of actin filament dynamics in cell motility. *Trends Cell Biol.* **2**, 219-221.
- Valentine, R. C., Shapiro, B. M. and Stadtman, E. R.** (1968). Regulation of glutamine synthetase XII. Electron microscopy of the enzyme from *Escherichia coli*. *Biochemistry* **7**, 2143-2152.
- Ward, S.** (1986). Asymmetric localization of gene products during the development of *Caenorhabditis elegans* spermatozoa. In *Gametogenesis and the Early Embryo* (ed. J.G. Gall), pp.55-75. Alan R. Liss, Inc., New York.
- Witke, W., Schleicher, M. and Noegel, A. A.** (1992). Redundancy in the microfilament system: abnormal development of *Dictyostelium* cells lacking two F-actin cross-linking proteins. *Cell* **68**, 53-62.

(Received 21 February 1994 - Accepted 3 June 1994)